

Tail of the distribution of fatalities in epidemics

Álvaro Corral^{1,2,3,4}

¹*Centre de Recerca Matemàtica, Edifici C,*

Campus Bellaterra, E-08193 Barcelona, Spain

²*Departament de Matemàtiques, Facultat de Ciències,*

Universitat Autònoma de Barcelona, E-08193 Barcelona, Spain

³*Barcelona Graduate School of Mathematics, Edifici C,*

Campus Bellaterra, E-08193 Barcelona, Spain

⁴*Complexity Science Hub Vienna, Josefstädter Straße 39, 1080 Vienna, Austria **

Abstract

The final size reached by an epidemic, measured in terms of the total number of fatalities, is an extremely relevant quantity. It has been recently claimed that the size distribution of major epidemics in human history is “strongly fat-tailed”, i.e., a power law asymptotically, which has important consequences for risk management. From the point of view of statistical physics and complex-systems modeling this is not an unexpected outcome, nevertheless, strong empirical evidence is also necessary to support such a claim. Reanalyzing previous data, we find that, although the fatality distribution may be compatible with a power-law tail, these results are not conclusive, and other distributions, not fat-tailed, could explain the data equally well. As an example, simulation of a log-normally distributed random variable provides synthetic data whose statistics are undistinguishable from the statistics of the empirical data. Theoretical reasons justifying a power-law tail as well as limitations in the current available data are also discussed.

*Electronic address: alvaro.corral@uab.es

I. INTRODUCTION

In complex systems, the statistical variability of the size of a phenomenon carries fundamental information about its underlying dynamics [1–5]. Recently, Cirillo and Taleb [6] have studied the size of major epidemics in human history, measured in number of fatalities. Using the figures from 72 epidemics, from the plague of Athens (429 BC) to the COVID-19 (still ongoing), they claim that the resulting fatality distribution is “extremely fat-tailed”, i.e., a power law, asymptotically (for very large values of the number of fatalities). Power-law distributions are an important paradigm in complex-systems science, representing the non-existence of characteristic scales and the divergence of moments. However, the empirical treatment of power-law data is a delicate issue [7–14], resulting in that the rigorous evidence in support of these distributions has been rather limited [13].

Reanalyzing the same epidemic data as Ref. [6], we find that, although the data may be compatible with an asymptotic power-law, there is no evidence in favor of this behavior, and other distributions, not fat-tailed, could explain the tail equally well or even better. In concrete, simulation of a tail coming from a truncated log-normal distribution provides data whose statistics are undistinguishable from the epidemic empirical data. Based on this log-normal tail we show how to provide a very rough estimate of the final expected size of the COVID-19 pandemic (which would turn out to be infinite in the case of a power law). We finally discuss under which physical circumstances one could expect a power-law tail for the size of epidemics, and the necessity of much better data. The present paper significantly extends and puts in a wider context the results of Ref. [15].

II. DATA AND COMPLETENESS

Most of the events analyzed in Ref. [6] come from the Wikipedia list of the biggest known epidemics caused by infectious diseases [16]. The list was complemented with a few more events, obtained from other sources (mainly Ref. [17]). Restricting to epidemics causing 1000 or more fatalities, this led to $N = 72$ events, from 429 BC to 2020 AD (CE); the resulting data is provided in Table 1 of Ref. [6], in concrete, in the 4th numeric column (average estimate). We will refer to this data as the original data set.

We are not aware of any study of completeness of such data. In order to address this

important point, we display the number of fatalities versus time of occurrence (beginning of the outbreak) in Fig. 1(a), where it can be clearly seen that the data looks certainly inhomogeneous. For example, between 735 AD (Japanese smallpox epidemic) and 1485 AD there is only one event, which happens to be the Black Death (largest event on record, with roughly 140,000,000 fatalities, starting in 1331).

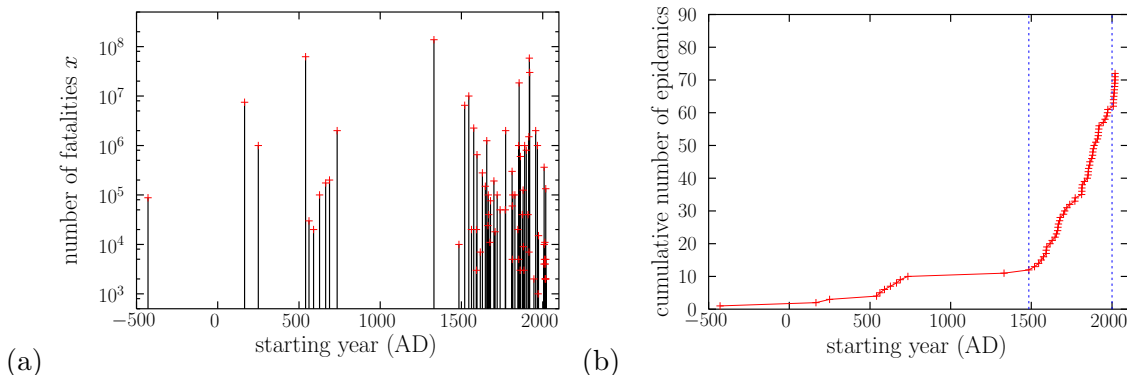


FIG. 1: Visualization of the original data set introduced in Ref. [6] and reanalyzed in the present paper. (a) Number of fatalities of each epidemic versus year of occurrence (beginning of the outbreak). (b) Cumulative number of epidemics versus year of occurrence. The slope yields the rate of occurrence. The vertical bars mark the window selected for the restricted data set also analyzed in the present paper. Both the inhomogeneity in time and the incompleteness in size become apparent.

Figure 1(b) confirms that the rate of occurrence of large epidemics seems to be highly inhomogeneous, from roughly 3 per century between 500 and 750 AD to just 1 in seven centuries (up to 1485) and to about 0.5 per year after 2000 AD. We associate this high variability mainly to the large incompleteness of the data and not to a wild variation of the occurrence of epidemics over the centuries.

Incompleteness can also be seen in the uneven distribution of the smallest events considered, i.e., out of the 17 epidemics below 10,000 fatalities, only 2 are contained in the first half of the data (from 429 BC to 1813). Including events below the completeness threshold can lead to important biases. Although in Ref. [6] it is claimed that a Jackknife resampling technique can account for incompleteness, it is obvious that resampling does not correct any bias present in the data (one must not get confused by the fact that Jackknife corrects the bias

of an estimator, which is clearly different from the bias arising from data incompleteness).

For this reason, in order to evaluate the impact of data incompleteness, in addition to analyze the raw data used in Ref. [6], we also consider a restricted data set, from 1485 to 2000 AD, which shows a higher homogeneity, with an average of 0.1 epidemics per year. This restricted data set consists of $N = 50$ epidemics. Note that the largest event, the Black Death, is not contained in this data set; thus, this provides a way to test the robustness of the results in front of the value of the most extreme event. This also eliminates ongoing epidemics (such as the COVID-19) from the analysis (except the HIV/AIDS pandemic).

A third data set, considered in Ref. [6], consist of rescaling the number of fatalities (of the original data set) by the whole world population at the time of the epidemic. This represents a procedure to take into account that the world population is far from stationary across history, and it is not the same to have 140 million of fatalities nowadays than in the Middle Ages (where the global population was around 400 million).

However, it is questionable why one should rescale by the world population and not by the local population (i.e., the population of Greece for the plague of Athens), and also why the scaling is linear with the total world population (for instance, in a simple branching process the size does not scale linearly with the size of the underlying tree, but with the square of the number of generations [18], and in general one has to take into account the so-called fractal dimension of the avalanches, see e.g. Ref. [19]). Nevertheless, we will also explore this simple rescaled data set, in order to test the robustness of the results.

III. DISTRIBUTIONS AND TAILS

The authors of Ref. [6] identify “fat-tailed” distributions with regularly varying distributions [14], defined by a complementary cumulative distribution function (or survival function [20], probability of being above x) given by $S_{fat}(x) = \ell(x)/x^\alpha$, with α the exponent (of $S_{fat}(x)$, and $\xi = 1/\alpha$ the tail index, measuring the “fatness” of the tail) and $\ell(x)$ an unspecified slowly varying function (for example, a function that tends to a constant when $x \rightarrow \infty$, but not only). Roughly speaking, a “fat-tailed” distribution becomes a power law asymptotically.

From the terminological point of view, the name “fat tail” becomes unfortunate, as it can be confused with the terms “long tail” and “heavy tail”, which denote different classes

of probability distributions. It is convenient to remember that fat-tailed distributions are subexponential distributions, which are long-tailed in their turn, which are heavy-tailed, but not the opposite [14]; in other words, in the previous four categories there is an implication chain that goes from left to right, but not from right to left.

In a nutshell, subexponential means that the probability of the sum of two independent variables is twice the probability of one of them; long-tailed means that the tail is unaffected by finite shifts ($S_{long}(x+c) \rightarrow S_{long}(x)$); and heavy-tailed is when the tail decays more slowly than any exponential [14]. A fundamental result of extreme-value theory is that fat-tailed distributions belong to the so-called Fréchet maximum domain of attraction, whereas heavy-tailed distributions that are not fat-tailed do not belong to such domain [14].

From an operational point of view, we define a power-law-tailed distribution (or just a power law, pl) as a distribution whose tail, defined by x above a lower-cut-off u (i.e., $x \geq u$), is given by the probability density

$$f_{pl}(x) = \frac{\alpha}{u} \left(\frac{u}{x}\right)^{1+\alpha}.$$

We will consider $f_{pl}(x) = 0$ for $x < u$, that is, all empirical data below u need to be disregarded [9]. Note that $f_{pl}(x)$ is the minus derivative of $S_{pl}(x) = (u/x)^\alpha$ (for $x \geq u$). Note also the difference between a fat tail, where the power-law may arise asymptotically, and a power-law tail, where the power-law arises above the cut-off u .

As an alternative description of the tail, we consider the example given by the truncated log-normal (ln) distribution, which is not fat-tailed but subexponential (and therefore long-tailed and heavy-tailed [14]). Its probability density is

$$f_{ln}(x) = \sqrt{\frac{2}{\pi}} \left[\operatorname{erfc} \left(\frac{\ln u - \mu}{\sqrt{2}\sigma} \right) \right]^{-1} \frac{1}{\sigma x} \exp \left(-\frac{(\ln x - \mu)^2}{2\sigma^2} \right), \quad (1)$$

for $x \geq u$ (and zero otherwise, so the truncation is for $x < u$), with μ and σ^2 the mean and variance of the underlying (untruncated) normal distribution, u the lower cut-off defining the starting point of the tail, and erfc the complementary error function [21].

The log-normal distribution has been an important competitor of the power law for the size distribution of structures and events in complex systems [13, 22, 23], due to the fact that it can be described as a sort of power law whose exponent is not constant but increases very slowly with x , when σ^2 is large. This is commonly found in log-log plots of empirical probability densities $f(x)$, which tend to show a slight downwards curvature (convexity for

physicists and concavity for mathematicians), as it would correspond to a slowly increasing exponent.

IV. DIRECT FIT OF THE TAIL

We proceed to the fitting of the power-law tail and the log-normal tail to the epidemic-size empirical data. Given the lower cut-off u , the fitting of the distributions is straightforward by maximum-likelihood estimation. However, the important point is precisely the determination of u , both when fitting the power-law and the log-normal tail (naturally, the value of u can be different in each case, and we will distinguish between u_{pl} and u_{ln} , respectively). Many different methods have been proposed for the determination of u in the case of power-law distributions (for bibliography, see Ref. [14]), including visual methods even [6].

We use the fitting procedure developed in Ref. [11], which is similar in spirit to the very-popular one of Ref. [9] but performing much better under controlled situations [10, 12, 14]. In essence, the procedure tries a wide range of possible values of u (50 per decade, equally spaced in log-scale) and selects the smallest one which gives an “acceptable” (greater than 0.20) p -value in a Kolmogorov-Smirnov goodness-of-fit test. The same method is applied to fit the truncated log-normal distribution [13].

A visualization of the resulting fits in comparison with the empirical estimations of the probability density (using logarithmic binning [11]) and of the survival function is provided in Fig. 2, using the original data set. It is apparent how both fits are very close to each other (the difference being much smaller than the uncertainty in the empirical values of the density) and also that the power law gives a probability higher than the log-normal for the most extreme events (as expected). The log-normal fit yields $u_{ln} = 1000$, $\mu = 10.43$ and $\sigma = 3.60$ (p -value 0.94; scale parameter $e^\mu \simeq 35,200$), whereas for the power law $u_{pl} \simeq 33,000$ and $\alpha = 0.34$ (p -value 0.21), see Table I.

The results for the restricted data set (years 1485-2000) are comparable. The graphical estimations of the distributions (not shown) look rather like the previous case. The power-law fit yields a close value of α , but a smaller u , as expected ($u_{pl} \simeq 14,000$), due to less undersampling of small x (Table I). The log-normal fit also leads to values of the parameters close to those of the original data set, as also shown in the table. In addition, for the rescaled

data set we find the same overall behavior (see the table once more). Thus, we conclude that the properties of the epidemic-size distribution are roughly the same for the original data set, for the restricted data set, and for the rescaled data set. This does not mean that incompleteness is not relevant, only that the degree of incompleteness is similar for the three data sets.

In this way, for the rest of the paper we concentrate on the original (not rescaled) data set for a more in-depth analysis, which will compare the statistical behavior of this empirical data with that of many realizations of the simulation of a truncated log-normal distribution, with $N = 72$ events and the values of the parameters u_{ln} , μ , and σ given above (and also in the first row of Table I).

One could argue that it would be fair to compare the fit of the truncated log-normal (which has finite mean, and is truncated from below) not with a power-law tail (with infinite mean) but with the ad-hoc tapering of the power-law tail used in Ref. [6]. We argue that there is no practical difference between both types of power laws in relation to the fitting of the empirical data.

Indeed, the authors of Ref. [6] introduced the change of variable

$$z = l - \Delta \ln \left(1 - \frac{x-l}{h-l} \right) \quad (2)$$

with h the total world population, l the smallest value taken by x , and $\Delta = h - l \simeq h$. The key point is that when $x = h$ then $z \rightarrow \infty$, whereas when $x \ll h$ then $x \simeq z$, and thus, a power law (untruncated from above) for z corresponds to a tapered power law for x , with a “sharp” truncation at $x = h$ (for what a strange thing a “sharp” truncation can be, see Ref. [24]).

The authors of Ref. [6] propose to transform the original data x into z , fit an power-law tail $f_{pl}(z)$ to z , and then transform back to obtain the tapered power-law (tpl) fit $f_{tpl}(x)$ of x . The resulting tpl distribution for x is given by $f_{tpl}(x) = f_{pl}(z)dz/dx$, with $dz/dx = \Delta/(h-x)$. Taking values $h = 7.7 \times 10^9$ (current world population, as suggested in Ref. [6]) and $l = 1000$, we get that the largest change in x is for the largest x , which is $x = 1.375 \times 10^8$, resulting in $z = 1.387 \times 10^8$ (and $dz/dx = 1.018$). Thus, the changes are so small that it yields the same results to fit a power law to the empirical data x or to the transformed data z , and then the fit given by $f_{tpl}(x)$ is, in practice, indistinguishable from what one obtains fitting directly the untruncated power law $f_{pl}(x)$ to x .

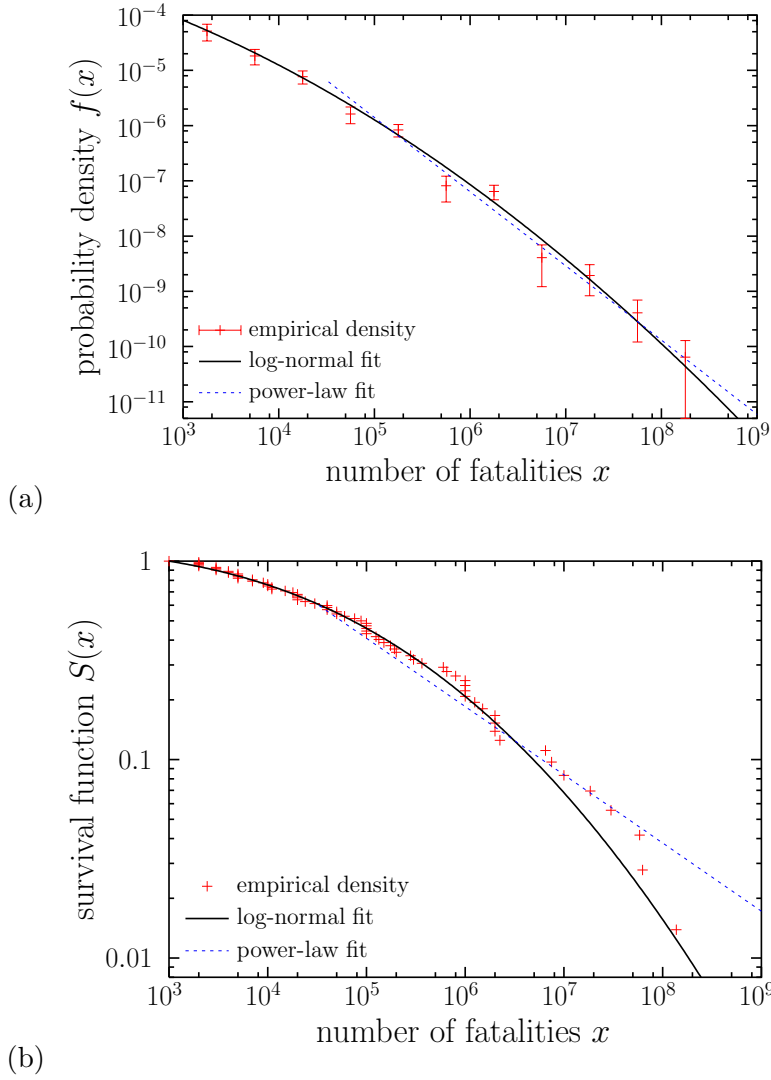


FIG. 2: Empirical distribution of the number of fatalities for each of the 72 historical epidemics in the original data set studied in Ref. [6]. A truncated log-normal fit and a power-law tail (starting at $u_{pl} \simeq 33,000$) are shown as well. (a) Probability density (empirical distribution obtained using logarithmic binning [11]). (b) Complementary cumulative distribution function (i.e., survival function).

TABLE I: Results from fitting a power-law tail (pl) and a truncated log-normal (ln) to the three data sets under consideration: (1) original, (2) restricted to the period 1485-2000 AD, and (3) original but rescaled by world population. x is number of fatalities except for (3), where it yields fatalities divided by world population at the time of the epidemic; x_{max} is the largest value of x on record; OM is the number of orders of magnitude covered by each fit, calculated as $\log_{10}(x_{max}/u)$; n is the number of events in the fitting range (above u); and p is the p -value of the fit. The results for the largest values of u for which the log-normal fit does not bring any improvement with respect the power-law fit, given by the log-CV test (cv), are also included.

	N	x_{max}	u_{pl}	OM _{pl}	n_{pl}	α_{pl}	p_{pl}	u_{ln}	OM _{ln}	n_{ln}	μ	σ	p_{ln}	u_{cv}	OM _{cv}	n_{cv}
1	72	138×10^6	33,100	3.6	43	0.344	0.20	1000	5.1	72	10.43	3.60	0.94	364,000	2.6	21
2	50	59×10^6	13,800	3.6	38	0.325	0.22	1000	4.8	50	11.01	3.13	0.85	600,000	2.0	15
3	72	0.35	5.2×10^{-5}	3.8	42	0.351	0.21	2.5×10^{-7}	6.1	72	-10.10	4.04	0.41	2.7×10^{-4}	3.1	28

V. MEAN-EXCESS SIZE AND MAXIMUM-TO-SUM RATIO

A. Mean-excess size

Reference [6] proposes two main ways to check fat-tailness. One of them uses the mean-excess function $\epsilon(u) = \langle x - u | x \geq u \rangle$, where the brackets denote expected value and the vertical bar denotes conditioning. This is the same as the expected residual size [25] (see also Ref. [26]) used in reliability theory and survival analysis, which characterizes a probability distribution in a way totally equivalent to $f(x)$ or $S(x)$, provided that the first moment of the distribution ($\langle x \rangle = \epsilon(0)$) is finite, which for a power-law tail happens when $\alpha > 1$. In this case, $\epsilon(u)$ should increase linearly with the lower cut-off u .

However, for a power-law tail with $\alpha < 1$ the first moment does not exist (is infinite), which implies that the mean-excess function does not exist either. Thus, in this case, the attempt of direct empirical estimation of $\epsilon(u)$ used in Ref. [6] (replacing the expected value in $\epsilon(u)$ by the sum for the empirical values) is futile, as one cannot estimate something that does not exist. Therefore, the empirical results of Ref. [6] are void of theoretical support in the case of power-law tails (which is the case considered in that reference).

Figure 3(a) shows this empirical estimation for the original data set of epidemic fatalities [6] and compares with the estimation of the mean-excess function for several realizations of log-normally simulated data (with the parameters obtained from the log-normal fit, Table I). Although there is considerable dispersion in the different realizations, there is no way to distinguish the empirical data from the log-normal simulations. Moreover, note that some degree of concavity (convexity for mathematicians) of the log-log plot seems to indicate that the empirical function would increase with u faster than any power of u , and thus faster than linearly (except for the four most extreme events).

B. Maximum-to-sum ratio

The other approach in Ref. [6] to fat-tailness uses the (partial) maximum-to-sum ratio (the maximum of the x -values divided by the sum of the values), with the data swept in chronological order. For $N \rightarrow \infty$ this ratio should tend to zero when the mean of the distribution is finite (as it happens with the log-normal but not with the power law when $\alpha < 1$, because both the maximum and the sum of a power law with $\alpha < 1$ scale superlinearly, as $N^{1/\alpha}$ [27, 28]).

We again compare the empirical data with the log-normal simulated data, sorting the simulated data in order that the ranks of the sizes (number of fatalities) follow the same temporal pattern as the empirical data (i.e., the largest simulated event is put on the 11th position, where the Black Death, the largest event on record, takes place in the original data, and so on).

The results, displayed in Fig. 3(b), show again that the behavior of the epidemic empirical data is indistinguishable from what is obtained for synthetic log-normal data (with a remarkable scattering), for which the max-to-sum ratio decreases with the number of data but without reaching zero. Thus, although the theory teaches us that the maximum-to-sum ratio tends to zero when $N \rightarrow \infty$ if the distribution has a finite mean, this convergence can be rather slow, as it happens with the log-normal distribution for the parameter values that describe the epidemic data.

In summary, the two methods used in Ref. [6] to provide evidence of fat-tailness for the description of the epidemic data are not able to rule out a log-normal tail.

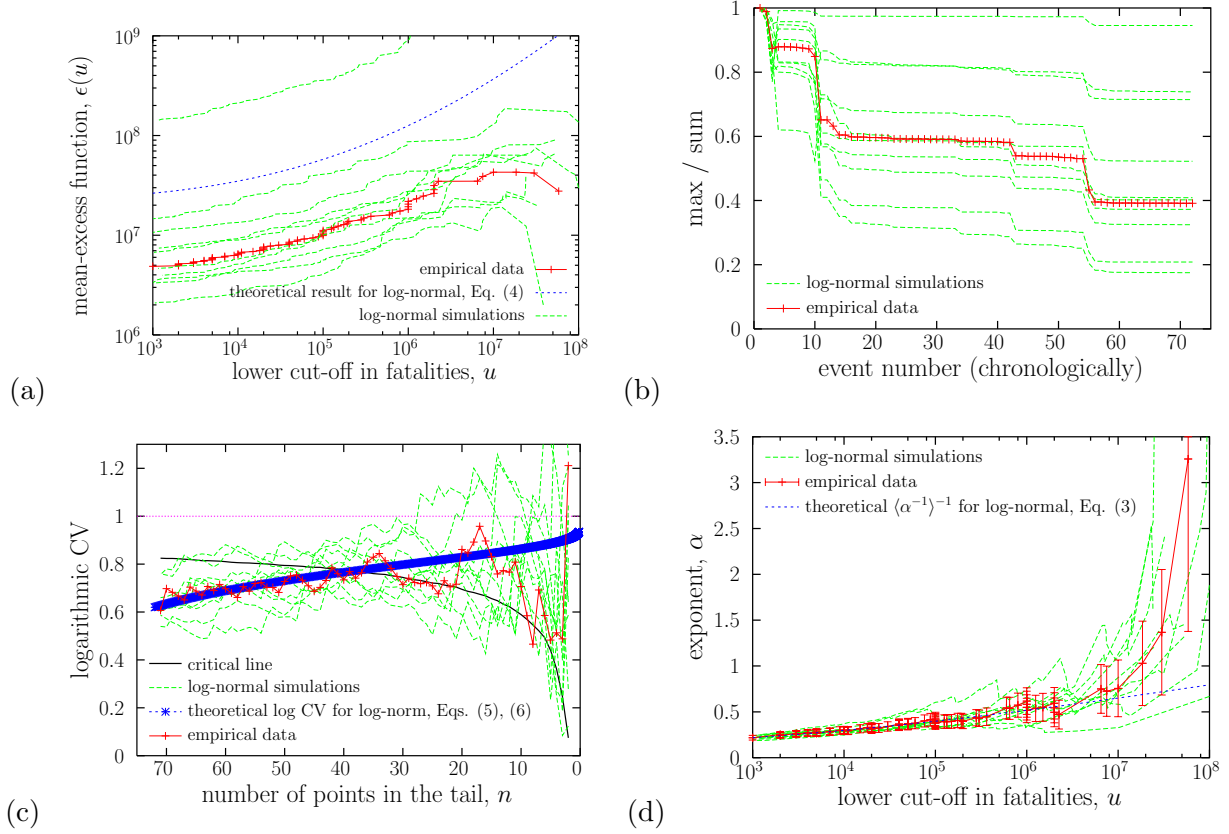


FIG. 3: Statistical properties of the number of fatalities of historic epidemics compared to those of 10 truncated log-normal synthetic samples with the parameters that fit the empirical data (Table I and Fig. 2). (a) Estimation of mean-excess function versus minimum size (lower cut-off) u ; the theoretical calculation for the fitted log-normal is also shown. (b) Maximum-to-sum ratio as a function of number of data, in chronological order. (c) Logarithmic coefficient of variation as a function of the number of points in the tail (those with $x > u$; note that the horizontal axis is reversed). The critical line corresponds to the 5th percentile, so the significance of the test is 0.05. The theoretical value of the logarithmic CV for the truncated log-normal is also shown. (d) Estimated power-law exponent α as a function of u , the error bars (α/\sqrt{n}) denote one standard deviation; the inverse of the expected value of α^{-1} calculated for truncated log-normally distributed data is also shown.

VI. LOGARITHMIC-CV TEST AND CHANGE OF APPARENT EXPONENT WITH CUT-OFF

A. Logarithmic coefficient-of-variation test

Now we expose complementary evidence that the truncated log-normal distribution can provide a good description for the tail of the epidemic data of Ref. [6]. In fact, the power law can be considered a particular case of the truncated log-normal (in the same way that the exponential is a particular case of the truncated normal distribution when $\sigma^2 \rightarrow \infty$ and $\mu \rightarrow -\infty$ with μ/σ^2 constant [29]). In this sense, a log-normal tail cannot provide a worse fit than a power law (it will be the same, or better). However, on the other hand, it may happen that this improvement in the fit is not significant, and then the power-law tail suffices for describing the data (as it has one parameter less than the log-normal). This is something that can be evaluated by a likelihood-ratio (LR) test [30].

Taking advantage of the fact that the LR between both distributions is a decreasing function of the logarithmic coefficient of variation (logarithmic CV) [29], this provides a very simple way to perform the LR test (without the need of performing maximum-likelihood fitting): critical values of the LR translate into critical values of the logarithmic CV. When this quantity is close enough to one, the test fails to reject the more parsimonious power-law hypothesis (although the log-normal is not rejected, but the gain it brings in likelihood is “superfluous”). When the LR departs significantly from one (from below), the power law is rejected in favor of the log-normal. This simple procedure provides a uniformly most powerful unbiased test between a power-law tail (null hypothesis \mathcal{H}_0) and a log-normal tail (alternative hypothesis \mathcal{H}_1 , containing \mathcal{H}_0 as a special case) [22, 29].

The test is performed for different values of the lower cut-off u , and the results, for the original data set, are displayed in Fig. 3(c). This shows that for the 21 largest epidemics, the power law tail is preferred (although remember that the log-normal tail is not rejected, as, being a generalization of the power law, with an additional parameter, cannot yield a worse fit). When the tail comprises more than 21 epidemics, the power-law is rejected in favor of the log-normal tail. The corresponding value of the cut-off u for this transition, u_{cv} , turns out to be at about 360,000 fatalities (Table I). In other words, the 21 epidemics with more than 360,000 fatalities are well described by a power law (the improvement brought

by the log-normal is not significant), but, including events below 360,000, the log-normal fit is significantly better (for the full range).

Applying the same procedure to the log-normally simulated data yields the same conclusion as in the previous section: the pattern obtained for the empirical data is indistinguishable from log-normal simulations, as also shown in Fig. 3(c). It is relevant to notice how, for log-normally distributed data (at least for the parameters in Table I, first row), there exists a tail that is indistinguishable from a power-law, and therefore the power-law is preferred, despite the simulated data are log-normal (by construction). This is an unavoidable consequence of the similarity between truncated log-normals and power laws, and implies that the fact that for the 21 largest epidemics the preferred fit is power law does not guarantee that the underlying distribution is not log-normal.

Note that in the case of the log-normally simulated data, as in the previous section, there is substantial scattering in the simulations. For the particular simulations shown in Fig 3(c) the range of points in the tail for which the power law is not rejected ranges from 3 to 68, with an average equal to 23 (with all cases of log-normally simulated data displaying a non-rejectable power-law tail). In addition, the logarithmic coefficient of variation of a truncated log-normal random variable can be exactly calculated (see the Appendix I, Eqs. (5) and (6)). This theoretical value is also shown in Fig. 3(c), using the fitted values of μ and σ to parameterize it. The agreement with the empirical data is remarkable, showing that the log-normal gives a better representation of the epidemic data than a simple power-law tail (and, as expected, the dispersion of the log-normal simulations is centered around the theoretical value).

B. Drift of the apparent power-law exponent

Assuming that a power law could describe the largest epidemics (in terms of fatalities), which would be the value of the corresponding power-law exponent α ? Above, for $u \simeq 33,000$, we report $\alpha = 0.34$, but for $u \simeq 360,000$ the maximum-likelihood estimation turns out to be larger: $\alpha = 0.45$. In fact, the estimated value of α is not stable at all, growing when the lower cut-off u increases, reaching $\alpha > 1$ for the highest values of u , see Fig. 3(d); that is, the fatness of the tail $\xi = 1/\alpha$ decreases systematically with u (this is already apparent in one of the plots of Ref. [6]), which prevents that one can establish a well-defined exponent

[31]. This increase of the apparent exponent α beyond one seems to contradict fat-tailness in general and the “extreme fat-tailness” claimed in Ref. [6] in particular.

Additionally, extreme-value theory [32] ensures that, for asymptotically large thresholds u (when the values of x are independent and identically distributed), the probability distribution of threshold exceedances $x - u$ tends to a generalized Pareto distribution (GPD). The parameter ξ of the GPD separates fat (power-law) tails (for $\xi > 0$, corresponding to the Fréchet maximum domain of attraction) from other tails ($\xi = 0$ or $\xi < 0$). But notice that, although ξ can be estimated from data using the Hill estimator (which is totally equivalent to the maximum-likelihood estimator for α we have used), the fact of obtaining a positive value of ξ does not mean that the data are fat tailed. The reason is that this calculation of ξ (or α) assumes that ξ is positive. In other words, one can never obtain a zero or negative value of ξ from the Hill estimator, which assumes fat-tailness by construction. So, contrary to what one may think, the positive values of ξ obtained in Ref. [6], and also here (Fig. 3(d)), do not provide evidence of fat-tailness.

Figure 3(d), in addition of showing the resulting exponents α as a function of u for the empirical data, also compares with the log-normally simulated ones. Once more, it is clear that the simulated data provides a pattern compatible with the empirical one, with an increase of the value of the exponent α when u increases (and with positive ξ , despite the log-normal does not belong to the Fréchet maximum domain of attraction). Indeed, this increasing behavior of the fitted exponent is what one expects from a log-normal distribution, for which the probability density appears as “convex” in a log-log plot. A power-law with $\alpha < 1$ does not provide such a systematic increase of α , in general.

We can go one step forward and provide a theoretical calculation of the value of α resulting from the fitting of a power-law tail to truncated log-normal data, in a spirit similar to that of Ref. [33]. The maximum likelihood estimation of α is simply the inverse of the sample mean of $\ln x - \ln u$ [11]. Assuming that x follows a truncated log-normal for $x \geq u$, with parameters μ and σ^2 , then $\ln x - \ln u$ follows a truncated normal distribution for $\ln x - \ln u \geq 0$, with parameters $\tilde{\mu} = \mu - \ln u$ and σ^2 . The expected value of such distribution gives, therefore, the expected value of the inverse of the estimation of the exponent (or the expected value of ξ), and can be easily calculated to be

$$\left\langle \frac{1}{\alpha} \right\rangle_{ln} = \langle \xi \rangle_{ln} = \mu - \ln u + \sigma \sqrt{\frac{2}{\pi}} \frac{e^{-(\ln u - \mu)^2 / (2\sigma^2)}}{\text{erfc}[(\ln u - \mu) / (\sqrt{2}\sigma)]} \quad (3)$$

[obtained also by direct integration of $(\ln x - \ln u)f_{ln}(x)$, from Eq. (1), see the Appendix I]. Figure 3(d) includes a comparison between the formula for $\langle \alpha^{-1} \rangle_{ln}^{-1}$ and the empirical estimation of α , as a function of u . The nearly perfect agreement between both is an extra argument in support of the plausibility of the truncated log-normality of the epidemic data.

VII. EXPECTED FINAL SIZE OF THE CURRENT COVID-19 PANDEMIC

Having in mind the limitations of the current study (incompleteness of historical records, information limited to just one value of a random variable per epidemic, mixture of totally different historical periods for the characteristics of epidemics...), an estimation of the expected final death toll from the current COVID-19 pandemic has to be understood only as a mathematical exercise. Nevertheless, this exercise can be very illuminating to learn about the counterintuitive properties of fat-tailed processes.

The question is: given that (at the time of the first submission of this article) the number of fatalities of the COVID-19 pandemic is $u \simeq 1,000,000$, which is the value we can expect for its (final) size? What we are asking for is $\langle x|x \geq u \rangle$, which is directly related to the mean-excess function $\epsilon(u)$ by $\langle x|x \geq u \rangle = \epsilon(u) + u$. The empirical estimation shown in Fig. 3(a) allows a direct calculation of this, turning out to be $\langle x|x \geq 10^6 \rangle \simeq 2.1 \times 10^7$. This is based just on the 18 historic events with $x \geq 10^6$.

We can try to use the diverse theoretical distributions, as arising from the fits, to try to improve this estimation. For a power-law distribution, we know that $\langle x|x \geq u \rangle_{pl} = \alpha u / (\alpha - 1)$; however, as we have already mentioned, this is only valid for $\alpha > 1$ [26]. For values of α below one (proposed in Ref. [6]), $\langle x|x \geq u \rangle_{pl}$ becomes infinite (although finite for an estimation of a finite sample and strongly dependent on N). In contrast, for the log-normal distribution, we can calculate the expected value from simulations (the existence of $\langle x|x \geq u \rangle_{ln}$ ensures convergence, in contrast to the power-law case with $\alpha < 1$); nevertheless, the convergence is rather slow, for $N = 10^6$ we obtain $\langle x|x \geq 10^6 \rangle_{ln} \simeq (1.09 \pm 0.04) \times 10^8$, which seems exaggeratedly large, but at least it is not infinite. In any case, this calculation clearly demonstrates that the risk posed by a log-normal tail should not be disregarded.

In fact, $\langle x|x \geq u \rangle$ can be calculated analytically for the truncated log-normal distribution,

starting from $\langle x|x \geq u \rangle = \int_u^\infty dx x f(x)/S(u)$. Let us denote $f_{ln}(x) = f(x; \mu, \sigma^2)$, then

$$x f(x; \mu, \sigma^2) = f(x; \mu + \sigma^2, \sigma^2) \frac{\text{erfc}\left(\frac{\ln u - \mu - \sigma^2}{\sqrt{2}\sigma}\right)}{\text{erfc}\left(\frac{\ln u - \mu}{\sqrt{2}\sigma}\right)} e^{\mu + \sigma^2/2}.$$

Identifying u with the lower cut-off of the distribution, $S(u) = 1$, and taking advantage that $f(x; \mu + \sigma^2, \sigma^2)$ has to be normalized we obtain

$$\langle x|x \geq u \rangle_{ln} = \frac{\text{erfc}\left(\frac{\ln u - \mu - \sigma^2}{\sqrt{2}\sigma}\right)}{\text{erfc}\left(\frac{\ln u - \mu}{\sqrt{2}\sigma}\right)} e^{\mu + \sigma^2/2}. \quad (4)$$

The value obtained from this formula for $u = 10^6$ is in total agreement with the results of the simulations. Subtracting u to the formula we obtain $\epsilon_{ln}(u)$, which is represented in Fig. 3(a) as a function of u .

One could be tempted to reduce the resulting value of $\langle x|x \geq 10^6 \rangle$ by introducing a much faster decay for very high values of x (e.g., at $x = h$). However, Ref. [24] shows that the results depend, obviously, not only on the value of h but also on the form of this fast decay, and the decay cannot be postulated ad-hoc. Note also that the estimation of $\langle x|x \geq u \rangle_{ln}$ from empirical or from simulated sampled is, naturally, a random variable (for fixed u). Figure 3(a) illustrates how the median of $\langle x|x \geq u \rangle_{ln}$ (around where most simulations gather) is close to the empirical result, but the previous calculation shows that the mean is far, and much higher.

The results in this subsection highlight the importance of the underlying statistical model, as the results may depend more on the assumptions contained in the model than on the empirical data. The estimations are crude because are based on crude data, just a one-dimensional random variable. Knowledge of the dynamics of the growth of the death toll with time until its final value x (on a daily, or monthly basis, etc.) for the historical data (in other words, knowledge of the “avalanche profile”) would provide more valuable information to improve the current estimation. Other limitations are explained in the final section.

VIII. DISCUSSION ON THE POSSIBILITY OF A FAT TAIL IN EPIDEMIC FATALITIES

The fact that the truncated log-normal distribution fits well the epidemic data is not a unique attribute of this distribution and probably other theoretical distributions, fat-tailed

or not, can do a similar good job; that is, there are candidate distributions, such as the stretched exponential or the Weibull, that could reproduce the empirical results well enough. This means that the “true” probability distribution describing the number of fatalities of epidemics cannot be established from a purely statistical analysis.

Fortunately, physical insights can shed light on this problem. Assuming a very simple (mean-field) model in which infections propagate following a Galton-Watson stochastic branching process [34–36], with a number of fatalities that is a fixed fraction of the number of infections (constant, deterministic infection fatality risk [37]), and identifying the branching ratio with the basic reproductive number, R_0 , it is immediate to see that $R_0 < 1$ leads to rather small epidemics (few number of fatalities, given by an exponential tail for x), whereas for $R_0 > 1$ two scenarios are possible starting from a single individual: again, few fatalities (“good-luck” case), or an infinite number of fatalities (“bad-luck”, in an infinite system). It is only at the critical point, $R_0 = 1$, where the number of fatalities is fat tailed, with an exponent $\alpha = 1/2$ (and this is known at least since the 1940s [34], provided that the distribution of contagions arising directly from one individual has a finite second moment).

For a sequence of historical epidemics, the distribution of the resulting number of fatalities will be a mixture of subcritical ($R_0 < 1$), critical, and supercritical ($R_0 > 1$) distributions, weighted by the distribution of R_0 , whose density is denoted here by $\rho(R_0)$; thus,

$$f(x) = \int f(x|R_0)\rho(R_0)dR_0.$$

For large x , only the critical and supercritical regimes need to be taken into account (as in subcriticality large values of x are totally negligible). Moreover, in a supercritical situation, whenever x reaches large enough values, one expects that social interventions to fight the epidemic are implemented; if these are effective the value of R_0 should decrease, slightly below one in the ideal case (and we should deal instead with R_T , with T the internal time of the epidemic). In this way, the contention of the epidemic triggers a feedback mechanism that, when x is large, sets the value of R_T close to the critical point of the model. The situation is that of self-organized critical phenomena [1, 38, 39]. Under these circumstances, one would expect a power-law tail for large x , with an exponent $\alpha = 1/2$ [36].

This shows in a simple scenario how a power-law tail is feasible, in agreement with Cirillo and Taleb [6]. Nevertheless, the situation just described is highly idealized, and the precise results would depend on the “natural” distribution of R_0 for contagious diseases and the

dynamics of R_T under mitigation measures. Finite-size effects should also be taken into account properly [18, 40].

In addition, needless to say, the Galton-Watson model is too simplistic, and other models, beyond mean field, may lead at least to a different value of the exponent α . For example, superspreading phenomena for which the number of contagions triggered directly by a single individual were power-law distributed [41] would lead, counterintuitively, to larger values of α ($\alpha > 1/2$, still fat tails, but thinner than in the Galton-Watson model [42]). In short, from a theoretical point of view, it seems reasonable that the epidemic size distribution is fat tailed, but, in any case, the hypothetical theoretical support does not make the supposed empirical evidence provided by Ref. [6] more valid.

IX. CONCLUSION

We have shown that there is not enough empirical evidence that the fatalities caused by epidemics along history follow a fat-tailed distribution. A log-normal tail (lacking fat-tailness) is able to replicate all sort of metrics used before [6] to support fat-tailness in the empirical record. For sure, some other not fat-tailed distributions could fit the data similarly well as the log-normal. What our work shows is the importance of considering alternative probability models when fitting heavy-tailed distributed data (which is different from fat-tailed data [14]), as well as the key role of computer simulations to contrast the validity of theoretical results when the number of data is not infinite.

Summarizing, log-normal tailed simulated data, in the same way as the empirical data, has: a mean excess size $\epsilon(u)$ that increases with a lower cut-off in size u ; a maximum-to-sum ratio that does not tend to zero as the number of events increases (up to $N = 72$); and a power-law tail exponent α that also increases with u (and which can be erroneously associated to a positive tail index ξ , despite the fact the log-normal belongs to the Gumbel maximum domain of attraction and should have $\xi = 0$ [32]; obviously, the calculation of ξ from the maximum-likelihood (Hill) estimator implicitly assumes $\xi > 0$). The agreement between empirical data and the log-normal simulations is not only qualitative but quantitative for the three metrics, although there is substantial scattering in the outcome of the simulation results (due to the small value of N).

Moreover, the uniformly most powerful unbiased test based on the logarithmic coefficient

of variation [22] shows that the power-law fit is preferred for the top 21 events of the empirical data, but this preference for a power-law tail is also shown for log-normal synthetic events; this is due to the well-known fact that the power law can be considered as a special case of a log-normal tail [22].

Our results also demonstrate that the risks brought by log-normally tailed phenomena can be enormous. Still, one may argue that from the point of risk management it is more conservative to take the power law (which gives a larger probability for the most extreme events) than the log-normal tail. This is true, but constitutes a different problem, which could be addressed even without any statistical modelling. For example, using the empirical data of Ref. [6], if an epidemic reaches 1000 fatalities then it has a non-negligible probability ($1/72 = 0.014$) of yielding 138 million fatalities. After reaching 10,000 fatalities this probability further increases (to $(1/72)/(55/72) \simeq 0.02$), and so on (of course, in this context extrapolation would not be possible and the probability of having an event with more fatalities than the Black Death cannot be computed). As the empirical data are rather incomplete, the previous numbers should not be considered truly reliable, but the same happens with the conclusions derived from any statistical model fitted to those data.

In fact, an important limitation when studying the distribution of fatalities in epidemics comes from the available data, not only because of the small sample size ($N = 72$ in the data of Ref. [6]), but also from the incompleteness of the data (with a bias in favor of very large events that resampling [6] cannot correct) and from the lack of homogeneity in time (with just one event, the Black Death, between 750 and 1450, and 11 events since 2008 in the data of Ref. [6]).

Notice that the data are inhomogeneous in an additional way: epidemics in the Middle Ages and in the 21st century are not comparable in the sense that they propagate differently and that the measures implemented for their contention should be more effective nowadays. If one mixes historical epidemic data with contemporary data what one obtains is, obviously, a mixture of distributions. This is not wrong *per se*, but one needs to have in mind for which reason one needs such knowledge in order to interpret the results properly. At the end, statistics derived from epidemic data of previous times have limited applicability nowadays (except if we faced pandemics with the same errors than in the Middle Ages).

In any case, one can dig a little in the existing records and find many more historical events. As an example, Villalba [43] reported several epidemics in Spain with more than

10,000 fatalities that are not considered in the data of Ref. [6] (these missing Spanish epidemics took place in 1283, 1394, 1490, 1564, 1589, 1637, 1726, 1741, 1784, and 1800). For sure, there is nothing special about Spain, and other countries can contribute more or less in the same way with more “hidden” epidemics. Nevertheless, the compilation of a reliable record for historical epidemics is something that should not be done by probabilists, statisticians, or physicists, and needs to be carefully undertaken by true epidemiologists and historians. We urge here for the necessity of such an important endeavor.

X. ACKNOWLEDGMENTS

I acknowledge Isabel Serra for discussions and Miguel Hernán and Diego Ramiro Fariñas for drawing my attention to Ref. [43]. And also support from projects FIS2015-71851-P and PGC-FIS2018-099629-B-I00 from Spanish MINECO and MICINN. I regret that it has been not possible to discuss these results with my colleague P. Puig, due to his problems with COVID-19.

XI. APPENDIX I: MOMENTS AND LOGARITHMIC COEFFICIENT OF VARIATION OF THE TRUNCATED LOG-NORMAL DISTRIBUTION

The logarithmic coefficient of variation of a random variable x above a threshold u is defined as the standard deviation of $\ln(x/u)$ divided by the expected value of $\ln(x/u)$, i.e.,

$$C = \frac{\sqrt{\langle \ln^2(x/u) \rangle - \langle \ln(x/u) \rangle^2}}{\langle \ln(x/u) \rangle},$$

where it is implicit that $x \geq u$. For the case of a truncated log-normal distribution with parameters μ and σ^2 , given by Eq. (1), the following change of variables $t = (\ln x - \mu)/\sigma$ leads to

$$C = \frac{\sigma \sqrt{\langle t^2 \rangle - \langle t \rangle^2}}{\mu - \ln u + \sigma \langle t \rangle},$$

and t turns out to follow a “tipified” truncated normal (tn) distribution with density

$$f_{tn}(t) = \frac{e^{-t^2/2}}{Z}, \text{ with } Z = \sqrt{2\pi} \times \frac{1}{2} \operatorname{erfc} \left(\frac{\ln u - \mu}{\sqrt{2}\sigma} \right),$$

for $t \geq (\ln u - \mu)/\sigma$. We call the distribution of t tipified because the parameters μ and σ have been transformed to take values zero and one, but these values are not the mean and

variance of t . Direct calculation of the moments of t is straightforward, leading to

$$\left\langle \ln \frac{x}{u} \right\rangle = \tilde{\mu} + \sigma \langle t \rangle = \tilde{\mu} + \sigma \frac{e^{-(\tilde{\mu}/\sigma)^2/2}}{Z}$$

with $\tilde{\mu} = \mu - \ln u$. This is the same as Eq. (3) for $\langle \alpha^{-1} \rangle_{ln}$. Also,

$$\langle \ln^2(x/u) \rangle - \langle \ln(x/u) \rangle^2 = \sigma^2(\langle t^2 \rangle - \langle t \rangle^2) = \sigma^2 \left(1 - \frac{\tilde{\mu}}{\sigma} \frac{e^{-(\tilde{\mu}/\sigma)^2/2}}{Z} - \frac{e^{-(\tilde{\mu}/\sigma)^2}}{Z^2} \right)$$

and therefore, the logarithmic coefficient of variation is given (for the truncated log-normal distribution) by

$$C = \frac{\sigma \sqrt{1 - \tilde{\mu} \sigma^{-1} e^{-(\tilde{\mu}/\sigma)^2/2} / Z - e^{-(\tilde{\mu}/\sigma)^2} / Z^2}}{\tilde{\mu} + \sigma e^{-(\tilde{\mu}/\sigma)^2/2} / Z}. \quad (5)$$

As μ and σ are fixed (determined from the fit of the empirical data), C depends only on $\ln u$. Figure 3(c) represents C as a function of the number of points in the tail, which, for each value of u , are estimated as $n = N S_{ln}(u)$, with $N = 72$ and

$$S_{ln}(u) = \frac{\text{erfc} \left(\frac{\ln u - \mu}{\sqrt{2}\sigma} \right)}{\text{erfc} \left(\frac{\ln 10^3 - \mu}{\sqrt{2}\sigma} \right)}. \quad (6)$$

XII. APPENDIX II: LOGARITHMIC COEFFICIENT OF VARIATION COMPUTATION IN R LANGUAGE

Although the codes used in this research have been developed in FORTRAN 77, we present a simple alternative in R for the logarithmic coefficient of variation. This can be used as a double check of our results. The program below simulates a truncated log-normal sample, draws the histogram using logarithmic binning (corresponding to Fig. 2(a)) and draws the logarithmic CV plot (corresponding to Fig. 3(c)). The (self-contained) R code follows

```
mu<-10.43; sigma<-3.60
N<-72; x[1:N]<-0
for (i in 1:N){
  while (x[i]<=1000) {
    x[i]<-exp(rnorm(1,mean=mu,sd=sigma)) }}

histog_log<-hist(log(x),probability = 'T',col='blue')
plot(exp(histog_log$mids),histog_log$density/exp(histog_log$mids),log='xy',type='p')

install.packages('ercv')
require(ercv)
cvplot(log(x),conf.level=0.85)
```

The R package `ercv`, used to draw the log CV plot, was published in Ref. [44].

-
- [1] P. Bak. *How Nature Works: The Science of Self-Organized Criticality*. Copernicus, New York, 1996.
 - [2] M. Mitzenmacher. A brief history of generative models for power law and lognormal distributions. *Internet Math.*, 1 (2):226–251, 2004.
 - [3] M. E. J. Newman. Power laws, Pareto distributions and Zipf’s law. *Contemporary Physics*, 46:323–351, 2005.
 - [4] D. Sornette. *Critical Phenomena in Natural Sciences*. Springer, Berlin, 2nd edition, 2004.
 - [5] S. Thurner, R. Hanel, and P. Klimek. *Introduction to the Theory of Complex Systems*. Oxford University Press, New Delhi, 2018.
 - [6] P. Cirillo and N. N. Taleb. Tail risk of contagious diseases. *Nature Phys.*, 16:606–613, 2020.
 - [7] E. P. White, B. J. Enquist, and J. L. Green. On estimating the exponent of power-law frequency distributions. *Ecol.*, 89:905–912, 2008.
 - [8] H. Bauke. Parameter estimation for power-law distributions by maximum likelihood methods. *Eur. Phys. J. B*, 58:167–173, 2007.
 - [9] A. Clauset, C. R. Shalizi, and M. E. J. Newman. Power-law distributions in empirical data. *SIAM Rev.*, 51:661–703, 2009.
 - [10] A. Corral, F. Font, and J. Camacho. Non-characteristic half-lives in radioactive decay. *Phys. Rev. E*, 83:066103, 2011.
 - [11] A. Deluca and A. Corral. Fitting and goodness-of-fit test of non-truncated and truncated power-law distributions. *Acta Geophys.*, 61:1351–1394, 2013.
 - [12] Hanel R., Corominas-Murtra B., Liu B., and Thurner S. Fitting power-laws in empirical data with estimators that work for all exponents. *PLoS ONE*, 12(2):e0170920, 2017.
 - [13] A. Corral and A. González. Power law distributions in geoscience revisited. *Earth Space Sci.*, 6(5):673–697, 2019.
 - [14] I. Voitalov, P. van der Hoorn, R. van der Hofstad, and D. Krioukov. Scale-free networks well done. *Phys. Rev. Research*, 1:033034, 2019.
 - [15] A. Corral. Scientific comment on “Tail risk of contagious diseases”. *arXiv*, 2007.06876, 2020.
 - [16] Wikipedia. List of epidemics. https://en.wikipedia.org/wiki/List_of_epidemics.
 - [17] ListFist. List of epidemics compared to coronavirus. <https://listfist.com/list-of-epidemics->

compared-to-coronavirus-covid-19.

- [18] A. Corral, R. Garcia-Millan, N. R. Moloney, and F. Font-Clos. Phase transition, scaling of moments, and order-parameter distributions in Brownian particles and branching processes with finite-size effects. *Phys. Rev. E*, 97:062156, 2018.
- [19] A. Corral and M. Paczuski. Avalanche merging and continuous flow in a sandpile model. *Phys. Rev. Lett.*, 83:575–578, 1999.
- [20] Note that the name survival or survivor function can be confusing. It makes a lot of sense when the random variable is a failure time or a lifetime, but not when we are dealing with other variables, as fatalities. Then, the interpretation of the survival function here cannot be the same as in reliability theory and survival analysis.
- [21] M. Abramowitz and I. A. Stegun, editors. *Handbook of Mathematical Functions*. Dover, New York, 1965.
- [22] Y. Malevergne, V. Pisarenko, and D. Sornette. Testing the Pareto against the lognormal distributions with the uniformly most powerful unbiased test applied to the distribution of cities. *Phys. Rev. E*, 83:036111, 2011.
- [23] A. Corral, F. Udina, and E. Arcaute. Truncated lognormal distributions and scaling in the size of naturally defined population clusters. *Phys. Rev. E*, 101:042312, 2020.
- [24] A. Corral. Finite-size scaling versus dual random variables and shadow moments in the size distribution of epidemics. *arXiv*, 2011.04316, 2020.
- [25] J. D. Kalbfleisch and R. L. Prentice. *The Statistical Analysis of Failure Time Data*. Wiley, Hoboken, NJ, 2nd edition, 2002.
- [26] M. Schroeder. *Fractals, Chaos, Power Laws*. Freeman, New York, 1991.
- [27] J.-P. Bouchaud and A. Georges. Anomalous diffusion in disordered media: statistical mechanisms, models and physical applications. *Phys. Rep.*, 195:127–293, 1990.
- [28] A. Corral. Scaling in the timing of extreme events. *Chaos. Solit. Fract.*, 74:99–112, 2015.
- [29] J. del Castillo and P. Puig. The best test of exponentiality against singly truncated normal alternatives. *J. Am. Stat. Assoc.*, 94:529–532, 1999.
- [30] Y. Pawitan. *In All Likelihood: Statistical Modelling and Inference Using Likelihood*. Oxford UP, Oxford, 2001.
- [31] J. Baró and E. Vives. Analysis of power-law exponents by maximum-likelihood maps. *Phys. Rev. E*, 85:066121, 2012.

- [32] S. Coles. *An Introduction to Statistical Modeling of Extreme Values*. Springer, London, 2001.
- [33] E. K. H. Salje, A. Planes, and E. Vives. Analysis of crackling noise using the maximum-likelihood method: Power-law mixing and exponential damping. *Phys. Rev. E*, 96:042122, 2017.
- [34] T. E. Harris. *The Theory of Branching Processes*. Dover, New York, 1989.
- [35] M. Kimmel and D. E. Axelrod. *Branching Processes in Biology*. Springer-Verlag, New York, 2002.
- [36] A. Corral and F. Font-Clos. Criticality and self-organization in branching processes: application to natural hazards. In M. Aschwanden, editor, *Self-Organized Criticality Systems*, pages 183–228. Open Academic Press, Berlin, 2013.
- [37] A. L. Hill. The math behind epidemics. *Phys. Today*, 73(11):28–34, 2020.
- [38] S. Zapperi, K. B. Lauritsen, and H. E. Stanley. Self-organized branching processes: Mean-field theory for avalanches. *Phys. Rev. Lett.*, 75:4071–4074, 1995.
- [39] N. W. Watkins, G. Pruessner, S. C. Chapman, N. B. Crosby, and H. J. Jensen. 25 years of self-organized criticality: Concepts and controversies. *Space Sci. Rev.*, 198:3–44, 2016.
- [40] R. Garcia-Millan, F. Font-Clos, and A. Corral. Finite-size scaling of survival probability in branching processes. *Phys. Rev. E*, 91:042122, 2015.
- [41] F. Wong and J. J. Collins. Evidence that coronavirus superspreading is fat-tailed. *Proc. Natl. Acad. Sci. USA*, 117(47):29416–29418, 2020.
- [42] A. Saichev, A. Helmstetter, and D. Sornette. Power-law distributions of offspring and generation numbers in branching models of earthquake triggering. *Pure Appl. Geophys.*, 162:1113–1134, 2005.
- [43] J. de Villalba. *Epidemiología española o Historia cronológica de las pestes, contagios, epidemias y epizootias que han acaecido en España desde la venida de las cartagineses hasta el año 1801*. Imprenta de Fermín Villalpando, Madrid, 1803.
- [44] J. del Castillo, I. Serra, M. Padilla, and D. Moriña. Fitting Tails by the Empirical Residual Coefficient of Variation: The ercv Package. *R Journal*, 11(2):56–68, 2019.